Ultrabroadband AlGaAs/CaF$_2$ semiconductor saturable absorber mirrors

S. Schön,[a)] M. Haiml, and U. Keller
Institute of Quantum Electronics, Swiss Federal Institute Zurich, ETH-Hönggerberg HPT, CH-8093 Zurich, Switzerland

Ultrabroadband semiconductor saturable absorber mirrors (SESAMs) are required to support self-starting sub-10-fs-pulse generation with Ti:sapphire lasers. Conventional $Al_xGa_{1-x}As/AlAs$ SESAMs are limited by the reflection bandwidth of about 60 nm of the bottom Bragg mirror. In this letter, we demonstrate a GaAs saturable absorber which is epitaxially grown on CaF$_2$ using molecular-beam epitaxy. Even though the difference of the thermal expansion coefficient is very large, we were able to demonstrate good modulation depth with small nonsaturable losses. This is interesting for ultrabroadband SESAMs because the large refractive-index difference between CaF$_2$ and $Al_xGa_{1-x}As$ results in very broadband $Al_xGa_{1-x}As/CaF_2$ Bragg mirrors extending over about a 400-nm-wide reflection bandwidth for a center wavelength of 850 nm. © *2000 American Institute of Physics.* [S0003-6951(00)04332-1]

Semiconductor saturable absorber mirrors (SESAMs) have been extensively used for passive pulse generation in solid-state lasers.[1,2] However, $Al_xGa_{1-x}As/AlAs$ Bragg mirrors limited the pulse generation with Ti:sapphire lasers to as short as 34 fs.[3] In this case, a single GaAs quantum-well layer was directly imbedded into an $Al_xGa_{1-x}As/AlAs$ Bragg mirror. Such a SESAM was later also referred to as a saturable Bragg reflector.[4] A different SESAM design, i.e., a high-finesse antiresonant Fabry–Pérot saturable absorber (AFPSA), was able to reduce the $Al_xGa_{1-x}As/AlAs$ Bragg mirror bandwidth limitation and supported 19 fs.[5] In the latter case, the SESAM consists of a lower $Al_xGa_{1-x}As/AlAs$ Bragg mirror, a GaAs saturable absorber layer, and a SiO$_2$/TiO$_2$ top reflector with a reflectivity of 96%. This reflector has a larger reflectivity bandwidth than the lower Fabry–Pérot mirror because the reflectivity bandwidth of Bragg mirrors increases rapidly with the ratio of the refractive indices of the materials forming the mirror (compare Figs. 1 and 2). The GaAs absorber layer thickness is adjusted for antiresonance of the Fabry–Pérot at the center wavelength of the 19 fs pulse. The free-spectral range of the Fabry–Pérot is then large enough and gives no bandwidth limitations to the device. In addition, the bandwidth limitation of the lower $Al_xGa_{1-x}As/AlAs$ Bragg mirror is reduced by the broadband high-reflective SiO$_2$/TiO$_2$ top reflector, which results in shorter pulses. So far, even shorter pulses were only obtained when the lower $Al_xGa_{1-x}As/AlAs$ Bragg mirror was replaced by a silver mirror.[6–8] Since the semiconductor saturable absorber cannot be grown directly on a silver mirror by molecular-beam epitaxy (MBE), postgrowth processing was applied to fabricate a low-finesse AFPSA. Such devices then supported sub-6-fs pulses,[9] which are short pulses generated directly from a Ti:sapphire laser.[10] Methods have been and are continued to be explored to avoid postgrowth processing of ultrabroadband SESAMs. To overcome the refractive-index limitation of $Al_xGa_{1-x}As/AlAs$ Bragg mirrors (Fig. 1), we have investi-

gated fluoride heteroepitaxy to increase the refractive-index difference (Fig. 2). Recently, we have demonstrated crack-free broadband $Al_xGa_{1-x}As/CaF_2$ Bragg mirrors.[11,12] In this letter, we demonstrate that a GaAs saturable absorber can be MBE grown on a CaF$_2$ layer without significant degradation of the saturable absorber parameters relevant for passive model-locked solid-state lasers.

For broadband SESAMs based on Bragg mirror structures, a material pair is needed which (a) differs largely in their refractive indices, (b) can be epitaxially grown in stacks, and (c) allows for growth of a saturable absorber material on top of the Bragg mirror or embedded in the mirror. For the best choice of a material pair fulfilling these requirements, we have to look at the optoelectronic properties such as refractive index and band-gap energy, and material properties like lattice constant, stability on air, and intermixing. Figure 2 presents the refractive indices versus lattice constants of commonly used semiconductors and insulators. Material pairs only made of III–V semiconductors will provide small bandwidth since their refractive indices do not differ very much. Beside $Al_xGa_{1-x}As/AlAs$ Bragg mirrors mentioned above, ZnX (X=S, Se, and Te) mixed crys-
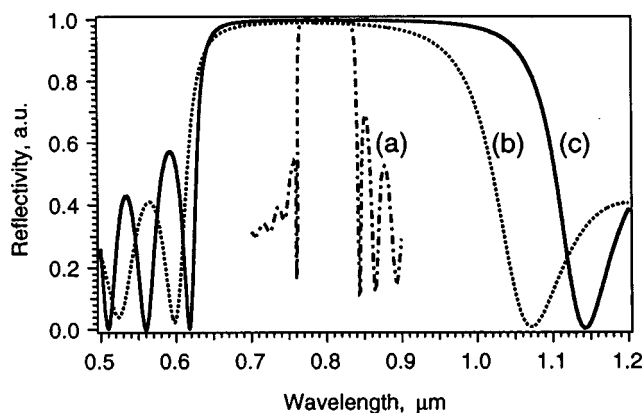

FIG. 1. Calculated reflectivity spectra for different Bragg mirrors: (a) 25 pairs $Al_{0.17}Ga_{0.83}As/AlAs$ on GaAs, (b) 4 pairs ZnTe/BaF$_2$ on ZnTe, and (c) 4 pairs $Al_{0.8}Ga_{0.2}As/CaF_2$ on GaAs.

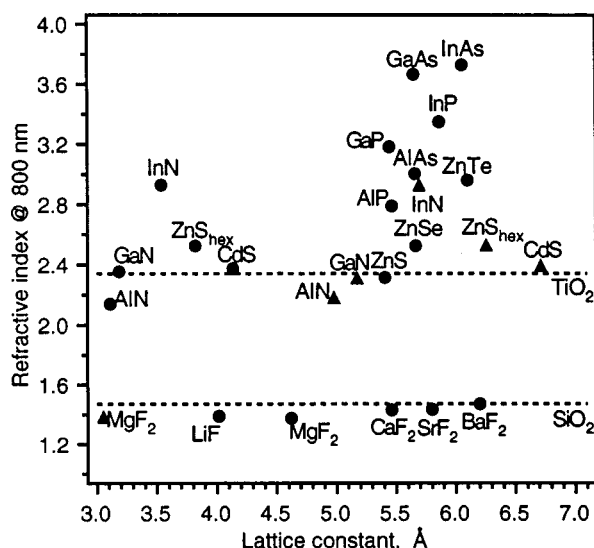[a)]Electronic mail: schoen@iqe.phys.ethz.ch

FIG. 2. Refractive indices (n, n_0 ●, n_e ▲) vs lattice constants (a, c) of commonly used semiconductors and insulators. The values for TiO_2 and SiO_2 are given by dotted lines since these materials are amorphous in broadband Bragg mirrors.

tals with additional Mg or Cd incorporated were used in distributed Bragg reflectors as well.[13] However, both III–V and II–VI Bragg reflectors face small spectral bandwidth and large numbers of mirror pairs to obtain reflectivities of >99%. An increase in refractive-index ratio can be provided with $ZnTe/BaF_2$ Bragg mirrors. The materials are nearly lattice matched and a high-reflection bandwidth of up to 310 nm can be obtained. However, Fig. 2 clearly shows that the highest difference in refractive indices is a combination of $Al_xGa_{1-x}As$ with a group-IIa fluoride, e.g., CaF_2. For the wavelength range of interest ($0.5–2\ \mu m$), fluorides are nonabsorbing and have no relevant dispersion. Most of them can be grown epitaxially by high-temperature evaporation. Some of the fluorides show a more (LiF) or less (BaF_2) hygroscopic behavior. Initially, $Al_xGa_{1-x}As/(Ca, Sr)F_2$ Bragg reflectors have been demonstrated with a 90% reflectance around a center wavelength of 870 nm for only three periods of layer pairs.[14] However, they suffered from serious crack formation after the epitaxy due to the thermal stress between both materials, which exhibit a large difference in their thermal expansion coefficient. We have demonstrated crack-free GaAs/fluoride Bragg mirrors using $CaF_2–BaF_2–CaF_2$ fluoride $\lambda/4$ layers with only thin CaF_2 parts.[15] Since the difference between the refractive indices of $CaF_2(1.42)$ and $BaF_2(1.46)$ (Fig. 2) is very small, the reflection at the $CaF_2–BaF_2$ interfaces can be neglected. BaF_2 can be grown epitaxially on CaF_2 and has a smaller stiffness constant, which was expected to help to overcome the crack problem caused by thermal mismatch strain. However, to reduce the complexity of the fluoride stack, we recently have demonstrated that low-temperature (LT) growth increases the maximum crack-free CaF_2 thickness. This allowed us to grow four-pair crack-free $Al_xGa_{1-x}As/CaF_2$ Bragg reflectors with >98% reflectivity at a center wavelength of 880 nm with a bandwidth of about 400 nm.[11] More recently, the interface roughness could be further improved using (111) substrate orientation compared to (100)-oriented growth.[12] This was

necessary for demonstration of a GaAs saturable absorber epitaxially grown on CaF_2.

At this point, it is important to note that there are other alternatives. Most low-index materials can be found among the oxides. Since it is rather difficult to obtain epitaxial growth with oxides, attempts have been made to combine Al_xO_y with GaAs by selective oxidation of $Al_xGa_{1-x}As$ with a high Al concentration. The oxidation process proceeded laterally to create buried-native-oxide layers. However, the oxidized area was restricted to a size of some $10\ \mu m^2$.[16] Recently, InAs-nanocrystallite-doped SiO_2 thin films were produced with rf sputtering.[17] However, the modulation depth was rather small and the saturation fluence very high (i.e., $25\ mJ/cm^2$), which is about 100–1000 times higher than that of typical SESAMs.[2,7] A large saturation fluence strongly increases the tendency for Q-switching instabilities in solid-state lasers,[18] and pushes the SESAM device closer to the material damage. In addition, the refractive indices of 2.34 (TiO_2) and 1.47 (SiO_2) limit the reflection bandwidth of SiO_2/TiO_2 Bragg mirrors to about 200 nm at a center wavelength of ≈800 nm. Chirped mirrors strongly increase the reflection bandwidth for a given material pair.[19,20] Thus, chirped SiO_2/TiO_2 mirrors supported pulses in the two-cycle regime with a reflection bandwidth of about 400 nm.[10] Chirped AlAs/GaAs semiconductor mirrors have been used to passively mode lock a Nd:glass laser.[21] However, to more fully explore the possible bandwidth, many more layers (i.e., in the order of 150 or more) have to been grown. This requires a very rigorous thickness control of each layer and the large number of layers results in increased absorption. Thus, the $Al_xGa_{1-x}As$/fluoride approach looks very interesting.

GaAs was chosen as the absorber material. A multilayer stack consisting of 57 nm GaAs sandwiched by 90 nm and 148 nm CaF_2 was optimized for maximum modulation depth of the absorber layer taking into account the standing-wave intensity pattern. This stack was grown by MBE on a GaAs(111) substrate. The growth was governed by a temperature-dependent lattice mismatch with up to 3.5% and by a large difference in the thermal expansion coefficients ($19.2\times10^{-6}/K$ for CaF_2 and $6.4\times10^{-6}/K$ for GaAs) causing strain in the layers. The (111) orientation is the preferred orientation of the fluorides and allows for strain relaxation by dislocation gliding in the fluoride layer. The drawback is the very small growth window for the (111)-oriented growth of GaAs. Homoepitaxial growth on (111)-oriented GaAs substrates is very sensitive to the absolute As pressure, the growth temperature, and the As/Ga flux ratio. In addition, the low free energy of the CaF_2 surface introduced mainly islanding, stacking faults, rotational twins, or microtwinning in the GaAs growth causing nonsaturable losses. Buffer-layer growth was carried out with growth interruptions on a ($\sqrt{19}\times\sqrt{19}$) reconstructed surface at 580 °C. CaF_2 overgrowth of GaAs at 620 °C provided a flat interface. The most challenging part of the growth was the heteroepitaxy of GaAs on CaF_2 due to the low-free-surface energy of CaF_2 and a low-As sticking coefficient. An impinging As flux was successfully applied before growth to increase surface wettability for the $Al_xGa_{1-x}As$ overgrowth of CaF_2. However, GaAs absorber layers grown under these conditions showed too fast recovery times due to high defect concentrations and
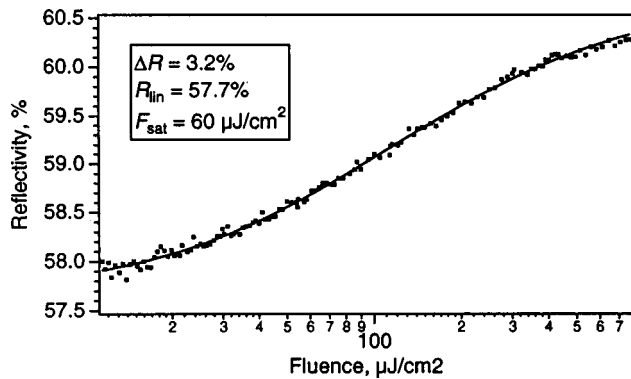
FIG. 3. Nonlinear reflectivity vs pulse energy fluence a of GaAs/CaF$_2$ multilayer stack (measured data, dots; fit function, full line).

additional nonsaturable losses caused by surface roughness. In contrast to the LT-grown or ion-implanted GaAs absorber layers used for conventional SESAMs, GaAs layers grown on CaF$_2$ at high temperatures already showed high defect concentration causing extremely fast recovery times and high nonsaturable losses. Impinging As flux on a CaF$_2$ surface decreased surface roughness but did also supply too much As supporting twin formation. In our studies, we found that GaAs growth is more sensitive to excessive As on the growth interface than Al$_x$Ga$_{1-x}$As. Therefore, we used electron-beam modification of the growth surface for the absorber growth. By breaking the Ca–F bonds with an electron beam, the exposed surface region became more attractive to Ga and As, improving growth and layer quality. More details on the growth will be reported elsewhere.[22]

The pulse-energy-dependent reflectivity at a center wavelength of 830 nm using approximately 150 fs pulses from a Ti: sapphire laser was measured to determine linear reflectivity R_{lin}, modulation depth ΔR, and saturation fluence F_{sat} (Fig. 3). The definition of R_{lin}, ΔR, and F_{sat} is given, for example, in Ref. 7. The temporal decay of the absorption was measured in a standard degenerate time-resolved pump–probe setup (Fig. 4). The area modified by
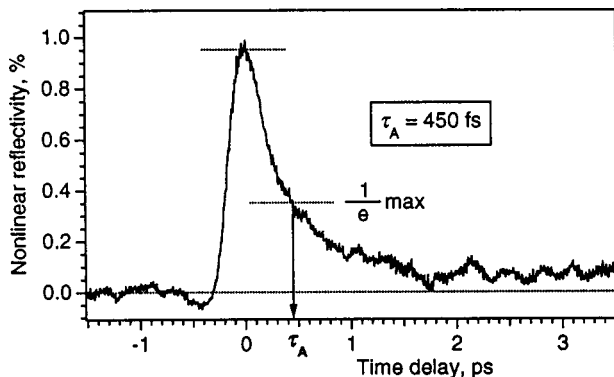
an electron beam during growth was found to have 57.7% in linear reflectivity and up to 3.5% in modulation depth, close to the calculated values of 58% and 4.5%, respectively (Fig. 3). A saturation fluence of 60 μJ/cm^2 was measured, which is low enough to avoid Q-switching instabilities in mode-locked solid-state lasers and material damage. For the unexposed regions, we obtained much higher losses in the linear reflectivity (R_{lin}=25%) and a modulation depth of approximately 1%. A constant recovery time of 450 fs was measured in all regions over the sample (Fig. 4). Such a fast recovery time makes the sandwiched GaAs layer an excellent choice for passively model-locked solid-state lasers.

In conclusion, we showed that GaAs grown on CaF$_2$ is an excellent choice for an absorber layer to be integrated in ultrabroadband Al$_x$Ga$_{1-x}$As/CaF$_2$ SESAMs. While other material combinations were discussed with respect to the fabrication of ultrabroadband SESAMs, III–V/fluoride stacks are very attractive and have provide a large high-reflection bandwidth.

[1] U. Keller, D. A. B. Miller, G. D. Boyd, T. H. Chiu, J. F. Ferguson, and M. T. Asom, Opt. Lett. **17**, 505 (1992).

[2] U. Keller, K. J. Weingarten, F. X. Kärtner, D. Kopf, B. Braun, I. D. Jung, R. Fluck, C. Hönninger, N. Matuschek, and J. Aus der Au, IEEE J. Sel. Top. Quantum Electron. **2**, 435 (1996).

[3] L. R. Brovelli, I. D. Jung, D. Kopf, M. Kamp, M. Moser, F. X. Kärtner, and U. Keller, Electron. Lett. **31**, 287 (1995).

[4] S. Tsuda, W. H. Knox, E. A. d. Souza, W. Y. Jan, and J. E. Cunningham, Opt. Lett. **20**, 1406 (1995).

[5] I. D. Jung, L. R. Brovelli, M. Kamp, U. Keller, and M. Moser, Opt. Lett. **20**, 1559 (1995).

[6] R. Fluck, I. D. Jung, G. Zhang, F. X. Kärtner, and U. Keller, Opt. Lett. **21**, 743 (1996).

[7] I. D. Jung, F. X. Kärtner, N. Matuschek, D. H. Sutter, F. Morier-Genoud, Z. Shi, V. Scheuer, M. Tilsch, T. Tschudi, and U. Keller, Appl. Phys. B: Lasers Opt. **65**, 137 (1997).

[8] Z. G. Zhang, T. Nakagawa, H. Takada, K. Torizuka, T. Sugaya, T. Mirua, and K. Kobayashi, Opt. Commun. **176**, 171 (2000).

[9] D. H. Sutter, G. Steinmeyer, L. Gallmann, N. Matuschek, F. Morier-Genoud, U. Keller, V. Scheuer, G. Angelow, and T. Tschudi, Opt. Lett. **24**, 631 (1999).

[10] G. Steinmeyer, D. H. Sutter, L. Gallmann, N. Matuschek, and U. Keller, Science **286**, 1507 (1999).

[11] Z. Shi, H. Zogg, and U. Keller, J. Electron. Mater. **27**, 55 (1998).

[12] S. Schön, H. Zogg, U. Keller, J. Cryst. Growth **201/202**, 1020 (1999).

[13] T. Tawara, M. Arita, K. Uesugi, and I. Suemune, J. Cryst. Growth **184/185**, 777 (1998).

[14] C. Fontaine, P. Requena, and A. Munoz-Yagüe, J. Appl. Phys. **68**, 5366 (1990).

[15] Z. Shi, H. Zogg, P. Müller, I. D. Jung, and U. Keller, Appl. Phys. Lett. **69**, 3474 (1996).

[16] P. W. Evans, J. J. Wierer, and N. Holonyak, J. Appl. Phys. **84**, 5436 (1998).

[17] I. P. Bilinsky, J. G. Fujimoto, J. N. Walpole, and L. J. Missaggia, Appl. Phys. Lett. **74**, 2411 (1999).

[18] C. Hönninger, R. Paschotta, F. Morier-Genoud, M. Moser, and U. Keller, J. Opt. Soc. Am. B **16**, 46 (1999).

[19] R. Szipöcs, K. Ferencz, C. Spielmann, and F. Krausz, Opt. Lett. **19**, 201 (1994).

[20] F. X. Kärtner, N. Matuschek, T. Schibli, U. Keller, H. A. Haus, C. Heine, R. Morf, V. Scheuer, M. Tilsch, and T. Tschudi, Opt. Lett. **22**, 831 (1997).

[21] R. Paschotta, G. J. Spühler, D. H. Sutter, N. Matuschek, U. Keller, M. Moser, R. Hövel, V. Scheuer, G. Angelow, and T. Tschudi, Appl. Phys. Lett. **75**, 2166 (1999).

[22] S. Schön, M. Haiml, M. Achermann, and U. Keller, J. Vac. Sci. Technol. B. **18**, 1701 (2000).

FIG. 4. Nonlinear reflectivity as a function of time measured with a standard degenerate pump–probe measurement at 830 nm with 150 fs pulses. The 1/e crossing time is 450 fs.